# Studies on Sequence Distributions in Acrylonitrile–Styrene Copolymers by Pyrolysis–Glass Capillary Gas Chromatography

**Tamio Nagaya, Yoshihiro Sugimura, and Shin Tsuge***

*Department of Synthetic Chemistry, Faculty of Engineering, Nagoya University, Nagoya 464, Japan.* *Received October 24, 1979*

ABSTRACT: High resolution pyrograms of acrylonitrile–styrene copolymers were obtained, using a microfurnace type pyrolyzer attached to a high-resolution glass capillary gas chromatograph. Almost complete assignment of the characteristic peaks on the pyrograms which cover the range up to the trimers was made by means of the directly coupled GC–MS system. The relative peak intensities were successfully interpreted in terms of the diad and the triad concentrations in the copolymer samples by applying the boundary effect theory on the formation of the products during the pyrolysis.

$^1$H NMR often provides very useful information about microstructures of copolymers. However, as for acrylonitrile–styrene copolymers (P(AN-*co*-St)), it has been limited mostly to the compositional[1,2] and qualitative analysis[3] since the associated NMR spectra of the copolymers are not sufficiently characteristic to allow quantitative interpretation of the microstructures. On the other hand, noise-decoupled $^{13}$C NMR was also applied to the structural study of the copolymers in terms of the triad concentrations in the copolymer chain.[4] In this case, however, the peak intensities of the triads are so small in comparison with the other peaks that the quantitative determination of the triad concentrations is accompanied by fairly large error, about ±10%. This reflects the difficulty in measuring widely differing intensities in the amplitude Fourier transform spectra.

On the other hand, the microstructures of P(AN-*co*-St) were also studied by pyrolysis–gas chromatography (PGC) in terms of the diad distributions along the copolymer chain.[5] In this study, however, only the peaks of the dimers and the hybrid dimers which barely separated by an ordinary packed column were utilized for the semiquantitative discussion on the diad sequence distributions.

In the present work, the high-resolution pyrograms of the P(AN-*co*-St) which cover the region up to the trimers and the hybrid trimers were obtained, using a glass capillary separation column which was attached to a microfurnace type pyrolyzer through a modified splitter.[6,7] The characteristic peaks on the pyrograms were identified by continuous monitoring, using a directly coupled PGC–mass spectrometry system. The relative peak intensities of the dimers and the hybrid dimers and those of the trimers and the hybrid trimers were quantitatively related to the associated diad and triad concentrations in the copolymer chain by applying the boundary effect theory to the formation of the characteristic products during the pyrolysis of the copolymer sample.[8]

## Experimental Section

**Samples.** Eleven P(AN-*co*-St) samples of different composition were prepared by the usual bulk radical polymerization at 50 °C in the presence of azobis(isobutyronitrile) (AIBN). The conversions were less than 10%. The composition of the samples was determined by elemental analysis and listed in Table I. The reactivity ratios, $r_{AN}$ = 0.04 and $r_{St}$ = 0.41, for the copolymer system were determined from the Fineman–Ross method.

**Pyrolysis–Gas Chromatographic Conditions.** The PGC system utilized is basically the same as that discussed previously.[6] A vertical microfurnace type pyrolyzer[9] was used to decompose the polymer samples. It was directly attached to the inlet port of a Shimadzu 7A gas chromatograph with a high-resolution glass capillary column (o.d. 0.9 mm × i.d. 0.3 mm × 50 m long) suspension coated with OV-101 and Silanox (325 mesh) from Shimadzu. In order to get high resolution, the active sites of the surface of the glass capillary column were treated with a dilute solution of PEG 20M, which was baked out at 250 °C for 30 h by passing nitrogen carrier gas and washed by chloroform prior to the final dynamic coating with OV-101. The column temperature was programmed from 50 to 250 °C at a rate of 4 °C/min. The splitting ratio was 55:1, and the flow rate of the carrier gas at the separating column was 1.0 mL/min. In order to prevent column deterioration from less volatile degradation products, Diasolid H (80–100 mesh) coated by 5% of OV-101 was packed in the dead volume of the splitter and its temperature was maintained at 250 °C.

A sample in the range 0.1–0.2 mg was accurately weighed and pyrolyzed at 510 °C under a flow of nitrogen carrier gas. The peak area of the pyrograms was integrated by a Shimadzu chromatopack E-1A integrator and peak identification was carried out using a Shimadzu LKB-2091 GC–MS system. Observations were repeated three times for each copolymer sample. The observed peak area was converted into the relative molar amounts according to the relative molar sensitivity of the components for the flame ionization detector (FID), using the calculated effective carbon numbers.[10]

As was described in our previous paper,[11] the relative standard deviation for the measurements of the associated monomer peaks from a P(MMA-*co*-St) sample was less than 1%.

Table I
Composition of Copolymer Samples

| sample no. | monomer feed ratio $z$ = [AN]/[St] | AN mol fraction in copolymer[a] |
|---|---|---|
| 1 | 0.053 | 0.102 |
| 2 | 0.176 | 0.233 |
| 3 | 0.333 | 0.312 |
| 4 | 0.538 | 0.367 |
| 5 | 0.818 | 0.408 |
| 6 | 1.222 | 0.440 |
| 7 | 1.857 | 0.468 |
| 8 | 3.000 | 0.496 |
| 9 | 5.667 | 0.534 |
| 10 | 19.000 | 0.633 |
| 11 | 32.333 | 0.694 |

[a] Determined by elemental analysis.

## Results and Discussion

Figure 1 shows the typical pyrograms of (A) polyacrylonitrile (PAN), (B) polystyrene (PSt), and (C) P(AN-*co*-St) at 510 °C. The main degradation products from PAN and PSt are monomers, dimers, and trimers, while the copolymers yield additional characteristic hybrid dimers and hybrid trimers. Comparing Figure 1 with the earlier pyrogram of P(AN-*co*-St),[5] which was separated up to dimer regions by an ordinary column, we noticed remarkable improvement in the resolution of the pyrograms obtained up to the trimer region. Peak assignments are listed in Table II, and the relative abundance of the deg-

0024-9297/80/2213-0353$01.00/0 

Table II
Peak Assignments of the Pyrograms

| | | | | | |
|---|---|---|---|---|---|
| 1 | $CH_2=CH$ \| CN | 10 | $CH_2-CH_2-C=CH_2$ \| \| Ph CN | 19 | $CH_2-CH_2-CH-CH=CH$ \| \| \| CN CN CN |
| 2 | $Ph-CH_3$ | 11 | $CH_2-CH_2-CH_2$ \| \| Ph CN | 20 | $CH=CH-CH-CH_2-CH-CH_3$ \| \| \| Ph CN CN |
| 3 | $Ph-CH=CH_2$ | 12 | $CH_2=C-CH_2-C=CH_2$ \| \| Ph CN | 21 | $CH_2-CH_2-CH-CH_2-CH_2$ \| \| \| CN CN CN |
| 4 | $Ph-C=CH_2$ \| $CH_3$ | 13 | $CH_2-CH_2-C=CH_2$ \| \| CN Ph | 22 | $CH_2-CH_2-CH-CH_2-C=CH_2$ \| \| \| CN CN Ph |
| 5 | $CH_2=C-CH_2-C=CH_2$ \| \| CN CN | 14 | $CH_2-CH_2-C=CH_2$ \| \| Ph Ph | 23 | $CH_2-CH_2-CH-CH_2-C=CH_2$ \| \| \| Ph Ph CN |
| 6 | $CH_2-CH=CH$ \| \| Ph CN | 15 | $CH_2=C-CH_2-CH-CH_2-C=CH_2$ \| \| \| CN CN CN | 24 | $CH_2-CH_2-CH-CH_2-C=CH_2$ \| \| \| CN Ph Ph |
| 7 | $CH=CH-CH_2$ \| \| Ph CN | 16 | $CH_2-CH_2-CH-CH_2-C=CH_2$ \| \| \| CN CN CN | 25 | $CH_2-CH_2-CN-CH_2-C=CH_2$ \| \| \| Ph CN Ph |
| 8 | $CH_2-CH_2-C=CH_2$ \| \| CN CN | 17 | $CH_2-CH_2-CH-CH_2-C=CH_2$ \| \| \| Ph CN CN | 26 | $CH_2-CH_2-CH-CH_2-C=CH_2$ \| \| \| Ph Ph Ph |
| 9 | $CH_2-CH_2-CH_2$ \| \| CN CN | 18 | $CH_2-CH_2-CH-CH_2-C=CH_2$ \| \| \| CN Ph CN | | |

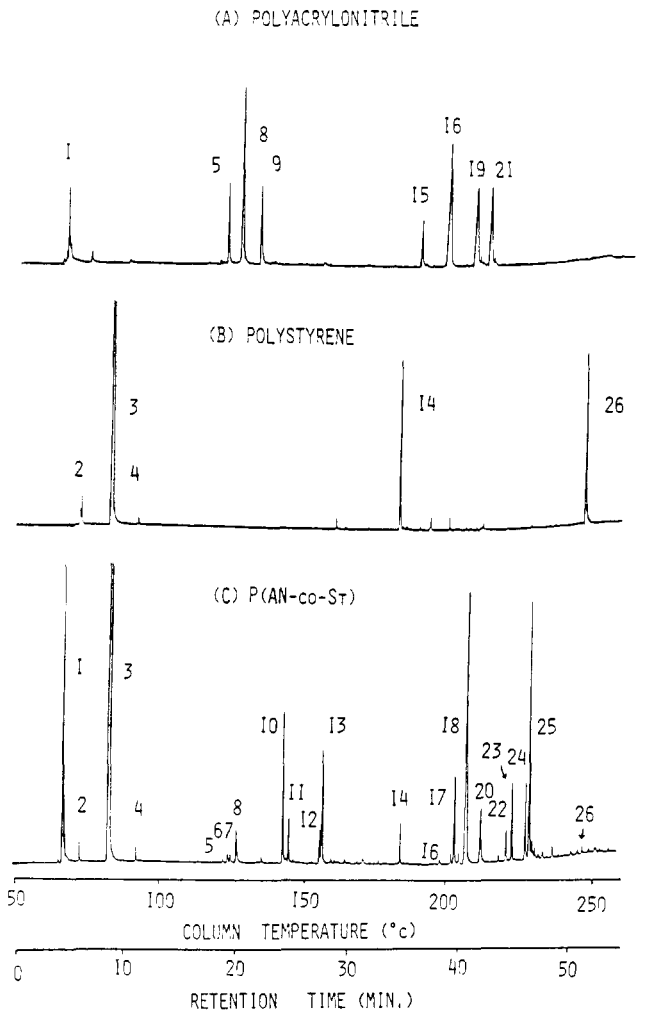


**Figure 1.** Typical pyrograms of (A) poly(acrylonitrile), (B) polystyrene, and (C) P(AN-*co*-St) (No. 8) at 510 °C. Peak assignments of the pyrograms are listed in Table II.

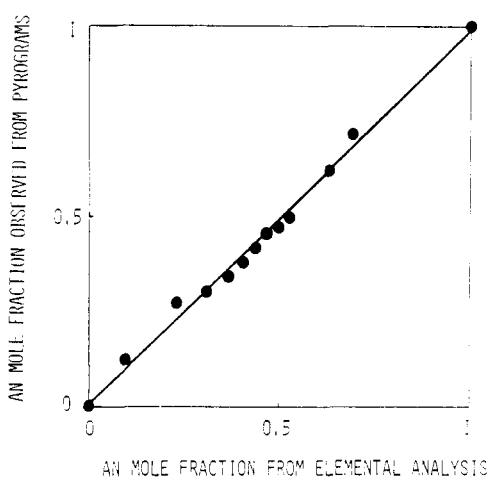


**Figure 2.** Relationship between the AN mole fraction observed from pyrograms and that from elemental analysis.

radation products is summarized in Table III. In these tables the degradation products which differ only in the carbon skeleton were assigned to the same dimer or trimer after making a correction for the molar sensitivity of each component for FID.

Here we should discuss the pyrolysis residue. The amount of residue for P(AN-*co*-St) increases as a function of the AN content. For example, the residue amounts to about 20% of the original copolymer sample for sample No. 8 (AN/St = 0.496/0.504). However, in the following, the contribution of the fairly high amount of pyrolysis residue was neglected by assuming that characteristic peaks up to trimers appearing on the pyrogram reflect the average molecular structures of the copolymer sample. This assumption is supported by the following experimental data. The observed total monomer unit yields $\sum A$ and $\sum S$ were calculated for each sample and listed in Table III. Figure 2 shows the relationship between $\sum A$ and the AN mole fraction of the original sample. The resulting fairly good linearity suggests that the observed peaks on the pyrograms should reflect the average molecular structures of the original copolymer samples almost quantitatively regardless of the copolymer composition.

**Theoretical Treatment for the Formation of Dimers and Trimers from the Copolymer Chain.** As was discussed in earlier papers,[5,8,12] there existed some function-

Table III
Relative Abundance of the Degradation Products

| sample no. | monomer | | dimer | | | trimer | | | | | | | total monomer unit[a] yield, % | |
|---|---|---|---|---|---|---|---|---|---|---|---|---|---|---|
| | A | S | AA | AS | SS | AAA | AAS | ASA | ASS | SAS | SSS | total | ΣA | ΣS |
| 1 | 6.8 | 68.3 | 0.1 | 4.3 | 5.7 | | 0.3 | 0.4 | 5.8 | 2.9 | 5.3 | 100.0 | 12.4 | 87.6 |
| 2 | 15.4 | 52.7 | 0.9 | 8.3 | 3.2 | 0.4 | 0.9 | 2.9 | 8.2 | 5.3 | 1.7 | 99.9 | 27.9 | 72.0 |
| 3 | 16.8 | 49.5 | 1.2 | 9.1 | 2.8 | 0.1 | 1.3 | 4.0 | 8.2 | 5.8 | 1.3 | 100.1 | 30.9 | 69.2 |
| 4 | 18.2 | 46.6 | 1.7 | 9.6 | 2.1 | | 1.7 | 5.6 | 7.5 | 6.3 | 0.8 | 100.1 | 34.2 | 65.9 |
| 5 | 20.1 | 43.3 | 2.3 | 9.6 | 1.6 | 0.1 | 2.2 | 7.6 | 6.4 | 6.4 | 0.5 | 100.1 | 38.1 | 62.0 |
| 6 | 21.4 | 40.1 | 2.8 | 9.8 | 1.3 | 0.2 | 3.3 | 9.3 | 5.2 | 6.3 | 0.3 | 100.0 | 41.5 | 58.5 |
| 7 | 22.4 | 38.2 | 3.2 | 9.6 | 1.1 | 0.5 | 4.4 | 10.3 | 4.0 | 6.1 | 0.2 | 100.0 | 44.1 | 55.9 |
| 8 | 21.4 | 34.4 | 3.8 | 9.7 | 0.8 | 0.6 | 6.5 | 13.1 | 3.3 | 6.2 | 0.1 | 99.9 | 46.9 | 53. |
| 9 | 20.1 | 31.1 | 5.0 | 9.3 | 0.6 | 0.8 | 10.5 | 14.8 | 2.2 | 5.4 | 0.1 | 99.9 | 50.0 | 49.9 |
| 10 | 19.6 | 23.5 | 14.4 | 8.6 | 0.4 | 6.4 | 13.9 | 10.0 | 0.4 | 2.6 | 0.1 | 99.9 | 61.6 | 38.3 |
| 11 | 18.1 | 16.9 | 19.3 | 7.1 | 0.4 | 15.0 | 13.3 | 8.5 | 1.2 | 1.7 | | 100.0 | 71.5 | 28.5 |
| PAN | 7.1 | | 31.7 | | | 61.2 | | | | | | 100.0 | | |
| PSt | | 83.4 | | | 8.3 | | | | | | 8.3 | 100.0 | | |

[a] Total monomer unit yield is calculated from monomer unit yields of monomer, dimer, and trimer on the pyrogram and normalized as $\Sigma A = [\Sigma A/(\Sigma A + \Sigma S)]100$ and $\Sigma S = 100 - \Sigma A$.

Table IV
Definition of Formation Probability Constants

| polymer chain[a] | K | formed product | polymer chain[a] | K | formed product | polymer chain[a] | K | formed product |
|---|---|---|---|---|---|---|---|---|
| -AAAA- | $K_1$ | AA | -AAAAA- | $K_{11}$ | AAA | -ASASA- | $K_{21}$ | SAS |
| -AAAS- | $K_2$ | | -AAAAS- | $K_{12}$ | | -ASASS- | $K_{22}$ | |
| -SAAS- | $K_3$ | | -SAAAS- | $K_{13}$ | | -SSASS- | $K_{23}$ | |
| -AASA- | $K_4$ | AS | -AAASA- | $K_{14}$ | AAS | -AASSA- | $K_{24}$ | ASS |
| -AASS- | $K_5$ | | -AAASS- | $K_{15}$ | | -AASSS- | $K_{25}$ | |
| -SASA- | $K_6$ | | -SAASA- | $K_{16}$ | | -SASSA- | $K_{26}$ | |
| -SASS- | $K_7$ | | -SAASS- | $K_{17}$ | | -SASSS- | $K_{27}$ | |
| -ASSA- | $K_8$ | SS | -AASAA- | $K_{18}$ | ASA | -ASSSA- | $K_{28}$ | SSS |
| -ASSS- | $K_9$ | | -AASAS- | $K_{19}$ | | -ASSSS- | $K_{29}$ | |
| -SSSS- | $K_{10}$ | | -SASAS- | $K_{20}$ | | -SSSSS- | $K_{30}$ | |

[a] For example, from -AAAA- in the copolymer chain the AA fraction is liberated as the AA dimer by the formation probability constant $K_1$.

alities between the diad concentrations and the observed relative dimer yields for various vinyl type copolymers

$$Y_2(AA) = k_1P_2(AA) \quad (1)$$

$$Y_2(AS) = k_2P_2(AS) \quad (2)$$

$$Y_2(SS) = k_3P_2(SS) \quad (3)$$

where $P_2(\ )$ represents the diad concentration in the copolymer, $Y_2(\ )$ is the observed dimer yield ($Y_2(AA) + Y_2(AS) + Y_2(SS) = 1$), and $k_1$, $k_2$, and $k_3$ are the correction parameters.

Naturally, the same tendency should exist between the triad concentrations and the observed relative trimer yields[13]

$$Y_3(AAA) = k_4P_3(AAA) \quad (4)$$

$$Y_3(AAS) = k_5\{P_3(AAS) + P_3(SAA)\} \quad (5)$$

$$Y_3(ASA) = k_6P_3(ASA) \quad (6)$$

$$Y_3(ASS) = k_7\{P_3(ASS) + P_3(SSA)\} \quad (7)$$

$$Y_3(SAS) = k_8P_3(SAS) \quad (8)$$

$$Y_3(SSS) = k_9P_3(SSS) \quad (9)$$

where $P_3(\ )$ represents the triad concentration in the copolymer, $Y_3(\ )$ is the observed trimer yield ($Y_3(AAA) + Y_3(AAS) + Y_3(ASA) + Y_3(ASS) + Y_3(SAS) + Y_3(SSS) = 1$), and $k_4$–$k_9$ are the correction parameters.

Applying the boundary effect theory developed for vinyl type copolymers,[12] the ASA trimer, for example, can be liberated from the different environments in the copolymer chain, i.e., -AASAA-, -AASAS-, -SASAS-. Generally, the formation probabilities of an ASA trimer from the three different pentad sections in the chain should be different from each other. Therefore, as summarized in Table IV, the associated trimer formation probability constants for the ASA are defined as $K_{18}$, $K_{19}$, and $K_{20}$ for -AASAA-, -AASAS-, and -SASAS-, respectively. Thus, the observed trimer yield, $Y_3(ASA)$, can be written as follows:

$$Y_3(ASA) = K_{18}P_5(AASAA) + K_{19}P_5(AASAS) + K_{20}P_5(SASAS) \quad (10)$$

where, $P_5(\ )$ represents a pentad concentration of the copolymer. If the copolymer system obeys the statistical copolymerization theory, the pentad concentration can be expressed in terms of the monomer reactivity ratio ($r_A$ and $r_S$) and the initial monomer feed ratios, $z$ ($=F_A/F_B$), for copolymerization. Therefore, combining eq 6 with eq 10, we can write the correction parameter $k_6$ as follows:

$$k_6 = \frac{r_A^2z^2K_{18} + 2r_AzK_{19} + K_{20}}{(r_Az + 1)^2} \quad (11)$$

Similarly, the correction parameters, $k$, can generally be

Table V
Determined Formation Probability Constants[a]

| | | |
|---|---|---|
| $K_1 = 1.65$ | $K_4 = 1.11$ | $K_8 = 0.90$ |
| $K_2 = 0.85$ | $K_5 = K_6 = 0.59$ | $K_9 = 0.17$ |
| $K_3 = 4.66$ | $K_7 = 1.65$ | $K_{10} = 0.94$ |
| $K_{11} = 1.83$ | $K_{14} = 1.52$ | $K_{18} = 1.76$ |
| $K_{12} = 1.92$ | $K_{15} = K_{16} = 1.28$ | $K_{19} = 0.53$ |
| $K_{13} = 1.01$ | $K_{17} = 11.68$ | $K_{20} = 1.28$ |
| $K_{21} = 0.41$ | $K_{24} = 4.01$ | $K_{28} = 0.49$ |
| $K_{22} = 0.89$ | $K_{25} = K_{26} = 0.62$ | $K_{29} = 0.10$ |
| $K_{23} = 1.54$ | $K_{27} = 1.74$ | $K_{30} = 0.62$ |

[a] $K_{m+1} = K_{m+2}$ in eq 13 was assumed for the simplicity.

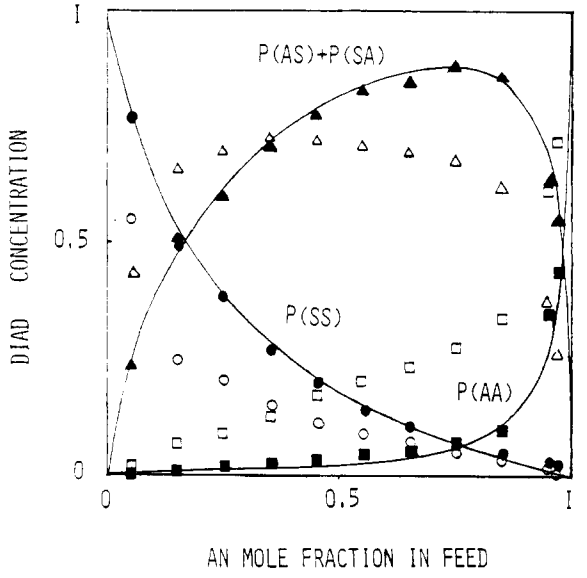


**Figure 3.** The concentration of diads in the AN-St copolymers: (○, △, □) observed $Y_2$ ( ); (●, ▲, ■) calculated $P_2$ ( ) from the probability formation constants method, using observed $Y_2$ ( ); (—) copolymerization theory $P_2$ ( ).

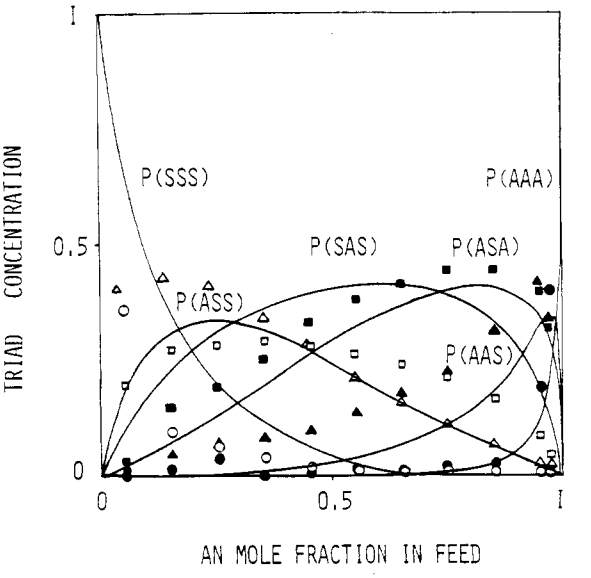


**Figure 4.** The concentration of triads in the AN-St copolymers: (○, △, □, ■, ▲, ●) observed $Y_3$(AAA), $Y_3$(AAS), $Y_3$(ASA), $Y_3$(ASS), $Y_3$(SAS), and $Y_3$(SSS), respectively; (—) copolymerization theory $P_3$( ).

expressed as functions of $r_A$, $r_S$, $z$, and the formation probability constants $K_1$–$K_{30}$: $l = 1$ for AA, $l = 11$ for AAA, $l = 18$ for ASA

$$k = \frac{r_A^2 z^2 K_l + 2r_A z K_{l+1} + K_{l+2}}{(r_A z + 1)^2} \tag{12}$$

$m = 4$ for AS, $m = 14$ for AAS, $m = 21$ for ASS

$$k = \frac{r_A z^2 K_m + z(K_{m+1} + r_A r_S K_{m+2}) + r_S K_{m+3}}{\frac{1}{2}(r_A z + 1)(z + r_S)} \tag{13}$$

$n = 8$ for SS, $n = 25$ for SAS, $n = 28$ for SSS

$$k = \frac{z^2 K_n + 2r_S z K_{n+1} + r_S^2 K_{n+2}}{(z + r_S)^2} \tag{14}$$

These equations suggest that the values of the formation probability constants can be experimentally determined, using the necessary sets of the observed $k$ values for solving the simultaneous equations. Once the probability constants are decided for the copolymer system, any sequence distribution of diad and triad in the copolymer chain can be estimated from the observed dimer and trimer yield, respectively.

The experimentally determined formation probability constants are summarized in Table V. As might be expected from the data in Table III for PAN and PSt, the formation constants for AA dimers are generally larger than those for SS dimers, reflecting the thermal degradation characteristics of the polymers. The same tendency can be seen for the formation of AAA and SSS trimers. However, it is very interesting to notice that among $K_1$–$K_3$, for AA dimer formation the AA diad both sides of which are neighbored by the counter monomer units, S, is most likely to be liberated as AA dimer while the AA diad which is surrounded by A and S has the least inclination to be the AA dimer.

Here, eq 12, 13, and 14 predict that the theoretical values of $K_1$, $K_{10}$, $K_{11}$, and $K_{30}$ should be equal to unity since PAN and PSt correspond to the extreme cases, $z \rightarrow \infty$ and $z \rightarrow 0$, respectively. However, the experimentally determined values are not exactly equal to unity. These results suggest that the relative values of the formation probability constants have much significance rather than the absolute

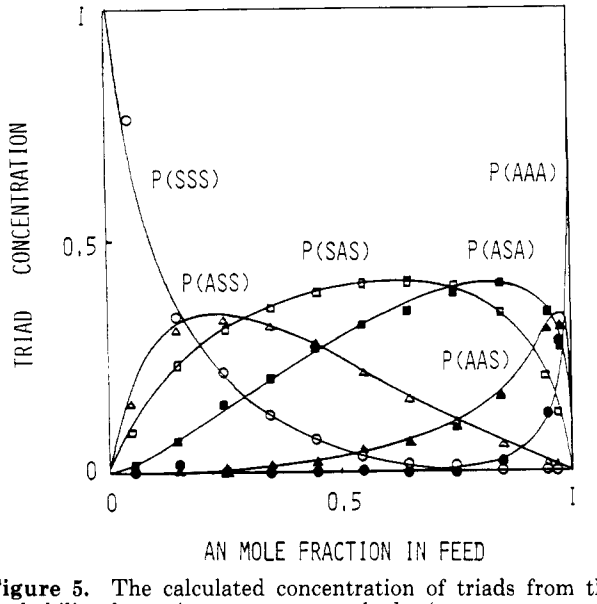


**Figure 5.** The calculated concentration of triads from the probability formation constants method: (○, △, □, ■, ▲, ●) calculated $Y_3$(AAA), $Y_3$(AAS), $Y_3$(ASA), $Y_3$(ASS), $Y_3$(SAS), and $Y_3$(SSS), respectively; (—) copolymerization theory $P_3$( ).

values. Thus from the relative values we can estimate the relative easiness of dimer or trimer formation from the copolymer chain during the thermal degradation.

As shown in Figure 3 the observed relative dimer yields $Y_2$( ) (○, △, □) were plotted against the copolymer compositions together with the theoretical curves of $P_2$( ) calculated by the usual copolymerization theory. Owing to the big differences in the thermal behavior to yield the corresponding dimers, these plots deviate considerably from the theoretical curves. However, when the experimentally determined dimer formation constants are taken into account, almost all the corrected values (●, ▲, ■) fall on the theoretical curves.

Similarly, the simple plot of the observed relative trimer yields, $Y_3$( ) against the copolymer compositions (Figure 4) shows significant deviations from the theory. The corrected plots (Figure 5), however, are in fair agreement with the plots from the theoretical values. These experimental data would support the effectiveness of the

boundary effect theory utilized in this work.

## References and Notes


(1) T. Takeuchi and M. Yamazaki, *Kogyo Kagaku Zashi*, **68**, 1478 (1965).
(2) B. K. Černicki, J. V. Mühl, Z. J. Janovic, and Z. K. Sliepčević, *Anal. Chem.*, **40**, 606 (1968).
(3) B. Patnaik, A. Takahashi, and N. G. Gaylord, *J. Macromol. Sci., Chem.*, **4**, 143 (1970).
(4) J. Schaefer, *Macromolecules*, **4**, 107 (1971).
(5) Y. Yamamoto, S. Tsuge, and T. Takeuchi, *Kobunshi Kagaku*, **29**, 407 (1972).
(6) Y. Sugimura and S. Tsuge, *Anal. Chem.*, **50**, 1968 (1978).
(7) S. Tsuge, T. Kobayashi, Y. Sugimura, T. Nagaya, and T. Takeuchi, *Macromolecules*, **12**, 988 (1979).
(8) T. Okumoto, S. Tsuge, Y. Yamamoto, and T. Takeuchi, *Macromolecules*, **7**, 376 (1974).
(9) S. Tsuge and T. Takeuchi, *Anal. Chem.*, **49**, 348 (1978).
(10) J. C. Sternberg, W. S. Gallaway, and D. T. L. Jones, "Gas Chromatography", N. Brenner et al., Ed., Academic Press, New York, 1960, p 231.
(11) S. Tsuge, Y. Sugimura, and T. Nagaya, *J. Anal. Appl. Pyrolysis*, in press.
(12) T. Okumoto, T. Takeuchi, and S. Tsuge, *Macromolecules*, **6**, 922 (1973).
(13) S. Tsuge, S. Hiramitsu, T. Horibe, M. Yamaoka, and T. Takeuchi, *Macromolecules*, **8**, 721 (1975).


# Molecular Parameters of Polymers Obtained from the Gibbs–DiMarzio Theory of Glass Formation


**Ivan Havlíček,*[1a] Vladimír Vojta,[1b] Michal Ilavský,[1a] and Jaroslav Hrouz[1a]**

*Institute of Macromolecular Chemistry, Czechoslovak Academy of Sciences, 162 06 Prague 6, Czechoslovakia, and Chemopetrol, Trojská 13, 180 00 Prague 8, Czechoslovakia.*

*Received September 21, 1979*


ABSTRACT: A numerical method of calculation of molecular parameters of the two-state Gibbs–DiMarzio (GD) model of glass formation using data on 15 polymers is presented. Experimental values of the glass transition temperature $T_g$, the change in the isobaric heat capacity $\Delta C_p$, the change in the temperature volume expansion coefficient $\Delta\alpha$, and the hypothetical equilibrium transition temperature $T_2$ (obtained from viscoelastic data) were used to calculate the GD parameters: flex energy $\epsilon$, hole energy $E_h$, and coordination number $z$. It was found that the energies $\epsilon$ and $E_h$ increase with $T_g$ of the polymer approximately linearly and do not differ too much from each other. The coordination number $z$ first decreases with increasing $T_g$ and then assumes a value of $z \approx 4.9$, thus supporting the favored theoretical value $z = 4$. The fractional free volume at $T_2$, $V_0(T_2)$, increases slightly with increasing $T_g$, while $V_0(T_g)$ increases less markedly, thus indicating that the free-volume concept of glass transition and the condition that configurational entropy equals zero at $T_2$ can both be valid simultaneously. The configurational entropy $S_c(T_g)$ and also the product $T_gS_c(T_g)$ decrease with increasing $T_g$. Theory predicts a rise in $\Delta\alpha(T)$ and a drop in $\Delta C_p(T)$ with increasing temperature, in accordance with the experiment. The Prigogine–Defay ratio determined by a combination of experimental and calculated thermodynamic quantitites at $T_g$ is higher than unity for all polymers, which suggests that the glass transition is a freezing-in process controlled by more than one order parameter.


Much attention has been devoted in the literature to theoretical and experimental problems of transition of the polymeric liquid into amorphous glass. This process is a kinetic one, as indicated by the dependence on the rate of cooling of both the glass transition temperature $T_g$ and the state of glass thus obtained. The Gibbs–DiMarzio statistical-mechanical theory (GD)[2-4] describes a case of hypothetical, infinitely slow cooling, during which a second-order transition should occur between the equilibrium liquid and equilibrium glass at a temperature $T_2$ situated approximately 50 K below the usually measured $T_g$. Oels and Rehage[5] criticize this concept and argue that glass transition is a freezing-in process and remains such also at $T_2$. Nose[6] chose a procedure which was somewhat different from GD and described glass transition on the basis of the hole theory of liquids. Tanaka[7] suggested an alternative partition function in order to demonstrate the effect of polymer conformations on the glass transition temperature.

The GD theory takes into account specific features of polymers, thus allowing one to express thermodynamic quantities as a function of the limited number of molecular parameters, namely, of flex energy $\epsilon$, hole energy $E_h$, coordination number $z$, degree of polymerization $x$, and number of rotatable groups per monomer unit $n_r$. Due to its compact form and comparatively simple mathematical relations, the GD theory is suited for comparison with experimental data. So far, comparisons have always been carried out by the use of simplified assumptions. Usually, it was assumed that $T_g$ equals $T_2$ and $z = 4$, and the calculations were performed with the following experimental data being known: (i) the change in the temperature volume expansion coefficient $\Delta\alpha$ (ref 3 and 8–10), (ii) the dependence of $T_g$ on the molecular weight (ref 11–14), and (iii) changes in the heat capacity at constant pressure $\Delta C_p$ and the isothermal compressibility of the polymer $\Delta\beta$ (ref 15).

The assumptions just outlined allow one to reduce the number of looked-for parameters of the theory usually to one or two, that is, flex energy $\epsilon$ and hole energy $E_h$. Conclusions following from these comparisons were then affected by initial assumptions: for instance, the fractional free volume at $T_g$, $V_{0g}$, yielded a universal value $V_{0g} \approx 0.036$, and it was found that $\epsilon/k = E_h/k$ (ref 8). In another analysis[16] the assumed validity of the Simha–Boyer empirical relation $\Delta\alpha T_g$ = constant and $T_g \approx T_2 + 30$–$50$ K gave $V_{0g} = 0.025$, $E_h/kT_2$ in the range 5–6, and $\epsilon/kT_2$ in the range 2.1–4, depending on $z$ (in the range $z = 4$–$12$). The dependence of $T_2$ on $z$, on the type of lattice, and on the flex energy $\epsilon$ in the case of one infinite molecule was investigated by Gordon et al.,[17] who came to the conclusion that Huggins' lattice model of the polymer solution approximates the number of possible arrangements of the molecule on the lattice more adequately than does the

0024-9297/80/2213-0357$01.00/0 